Available online at www.sciencedirect.com
SCIENCE DIRECT
Polymer 47 (2006) 2760–2771
polymer
www.elsevier.com/locate/polymer

Continuity development in polymer blends of very low interfacial tension

Prashant A. Bhadane [a], Michel F. Champagne [b], Michel A. Huneault [b], Florin Tofan [c], Basil D. Favis [a,*]

[a] *CREPEC, Department of Chemical Engineering, École Polytechnique de Montréal, 2900 Édouard Montpetit, P.O. Box 6079, Station Centre-Ville, Montréal, Qué., Canada H3C 3A7*
[b] *Industrial Materials Institute, National Research Council of Canada, 75 de Mortagne Blvd., Boucherville, Qué., Canada J4B 6Y4*
[c] *Lavergne Group, 8800 Crescent 1, Ville d'Anjou (Montréal), Qué., Canada H1J 1C8*

Received 15 November 2005; accepted 17 January 2006
Available online 3 March 2006

Abstract

Phase continuity development and co-continuous morphologies are highly influenced by the nature of the interface in immiscible polymer blends. Blends of ethylene–propylene–diene terpolymer (EPDM) and polypropylene (PP) possess an interfacial tension of about 0.3 mN/m and provide an interesting model system to study the detailed morphology development in a very low interfacial tension binary system. A variety of blends with viscosity ratios of 0.2–5.0 and shear stresses of 11.7–231.4 kPa were considered. Using a variety of sophisticated morphology protocols it is shown that at low blend compositions, the dispersed phase actually exists as stable fibers of extremely small diameter of 50–200 nm and the continuity develops by fiber–fiber coalescence. An analysis using break-up times from Tomotika theory also supports the notion of highly stable dispersed fiber formation. These results challenge the current view of the dispersed phase as small spherical droplets. It is shown, under these conditions, that a seven-fold variation in the viscosity ratio has virtually no influence on % continuity or morphology, while a large change in the matrix shear stress from 11.7 to 90.9 kPa has an important effect on pore diameter. Both sides of the continuity diagram are studied and highly symmetrical continuity behavior is observed with composition. In fact a single master continuity curve is observed for these blends varying in viscosity ratio from 0.7–5.0 and with shear stresses from 11.7–90.9 kPa. Although the glass transition temperatures indicate that these materials are completely immiscible after melt mixing and cooling, it is shown that the blends demonstrate the morphological features of a partially miscible system. These results support a concept that the blend was partially miscible during melt blending, at which time the gross morphological features of the blend were developed, but becomes fully phase separated upon cooling. It appears that the quenching of the EPDM/PP blend from the melt is rapid enough to preserve the imprint of that partial miscibility on the gross blend morphology.

Keywords: Polymer blends; Co-continuous morphology

1. Introduction

Today, polypropylene (PP) is produced on a massive scale because of its versatile properties and for years now, the unfavorable low temperature brittleness of PP has been overcome by blending it with different elastomers. Ethylene–propylene–diene terpolymer (EPDM) has been found to be the most successful elastomer in blending with PP due to: the very low interfacial tension (σ) ($\approx$0.3 mN/m at 190 °C) [1–6] and the low glass transition temperature of EPDM (≈ -40 to -50 °C) [7–12]. Furthermore, the EPDM can be crosslinked, which opens up numerous advantages as a thermoplastic vulcanizate (TPVs) [13–16].

At low compositions in PP and when the viscosity ratio is near unity, the EPDM phase has been reported to form very fine dispersed spherical domains. Number average particle sizes as low as 0.2 μm have been reported in the literature for blends prepared via melt mixing [17–22] making this one of the finest blend morphologies reported in the polymer blend literature.

Many authors have reported EPDM/PP blends to be immiscible [7,19,23–28], however, the miscibility–immiscibility issue in this blend system is very complex and controversial. In the past, Lohse et al. [26], by small angle neutron scattering (SANS) and more recently Han et al. [28] by determining the solubility parameter through pressure–volume–temperature (*P–V–T*) properties measurement, demonstrated that unlike atactic-PP (aPP), EPDM is immiscible both in the melt and on cooling from the melt with isotactic-PP (*i*PP).

* Corresponding author. Tel.: +1 514 340 4711x4527; fax: +1 514 340 4159.
E-mail address: basil.favis@polymtl.ca (B.D. Favis).

0032-3861/$ - see front matter © 2006 Elsevier Ltd. All rights reserved.
doi:10.1016/j.polymer.2006.01.065

This is the case even when the ethylene content of the elastomer is as low as ca. 8%. However, recent similar SANS experiments carried out by Seki et al. [29] with deuterated-EPDM (unlike Lohse who used deuterated-PP) prepared with metallocene catalyst indicated that these blends are a homogeneous one-phase mixture in the melt.

Chen et al. [8] found EPDM/PP blends to be immiscible below an upper critical solution temperature (UCST) determined by the crystallization temperature curve and above a lower critical solution temperature (LCST) from cloud point measurements. Thus, these blends are miscible in the temperature range in between the UCST and LCST. Inaba et al. [30,31] have reported that immiscible EPDM/PP blends phase separate by a spinodal decomposition mechanism above their melting temperature. The crystallization takes place and proceeds in and through PP-rich domains without invoking the long-range rearrangement of PP molecules. These discussions demonstrate the complexity and controversial nature of the miscibility–immiscibility issue in EPDM/PP blends.

Recently, Marin et al. [32] studied the co-continuous morphology development in partially miscible poly(methyl methacrylate) (PMMA)/polycarbonate (PC) blends. Both polymers are amorphous in nature and possess an interfacial tension of 0.6 mN/m. In that work it was shown that, because of the partial miscibility, the blend demonstrated significantly different morphological features as compared to that reported for fully immiscible blends of low interfacial tension by Li et al. [33]. Marin et al. found that these partially miscible blends exhibited very fine dispersed phase morphologies, artificially high percolation thresholds, and attained co-continuity at higher than expected compositions of the minor phase. Furthermore, these blends demonstrated significant coalescence effects as a function of dispersed phase composition as compared to the highly stable morphologies observed for fully immiscible binary blends of low interfacial tension. Marin et al. carried out a detailed correction of the phase composition and continuity phenomena by treating the blend as a mixture of PMMA-rich and PC-rich phases. Once these corrections were carried out, the continuity phenomena in terms of percolation onset and attainment of co-continuity fell in line with the expected behavior for a low interfacial tension binary system.

Despite their commercial significance, detailed morphological studies of EPDM/PP blends are lacking in the literature. In particular, continuity development and co-continuity are virtually untreated for this blend system. Furthermore, this system provides an excellent view into the blend morphology development of systems with very low interfacial tension. This paper is the first of a series of works that will examine the morphology development in EPDM/PP blends in a highly detailed fashion. Future works will involve examination of continuity development and co-continuity in high viscosity ratio blends and the relationship of the final crosslinked morphology to the initial non-crosslinked morphological states.

2. Experimental procedures

2.1. Materials

Three EPDM elastomers with different Mooney viscosities and two different types of PP homopolymers with significantly different melt flow indexes were used in this study. The materials do not contain any fillers. The ethylene and diene content of all the grades of EPDM were kept as similar as possible to eliminate any effect of these variables on the study. All EPDM grades contain ethylidene norbornene (ENB) as the diene. A small amount (0.5 wt%) of Irganox B 225 antioxidant was added to the mixture to reduce the oxidative degradation of PP. Further details concerning the materials are given in Table 1.

2.2. Rheological characterization

The neat EPDM, and PP containing 0.5 wt% Irganox B 225 were compression molded at 190 °C in the form of disks for rheological characterization. The rheological characterization was carried out using a Bohlin constant stress rheometer (CSM) in the dynamic mode. The experiments were performed using a parallel plate geometry of 25 mm diameter, at 190 °C and under a nitrogen atmosphere. An oscillation mode at 0.1 Hz frequency was used to test the stability of the materials at the test temperature. Both PP homopolymers, after addition of an antioxidant, were found to be stable, however, all the grades of EPDM showed the tendency to crosslink (as indicated by the increase in viscosity over time). Thus, several samples were used to carry out rheological experiments, so as not to exceed the time window revealed by the time sweep test. A stress sweep was then performed from 0.3 to 2420 Pa to determine the region of linear viscoelasticity. The frequency sweep tests were performed in an experimental window permitted by the time and stress sweep tests.

2.3. Melt blending

PP, EPDM, and antioxidant were first dry blended in a beaker and the mixture was fed all together into the mixing chamber. The two polymers were melt blended using a Haake Rheomix 600 internal mixer equipped with a 69 cm^3 chamber and roller-type rotors for 8 min at 100 rpm and at 190 °C. Under these mixing conditions an average shear rate of 27 s^{-1}

Table 1
Characteristic properties of the materials

Polymer	Supplier	Given name	Molecular weights $\times 10^3$		Ethylene content (%)	ENB content (%)
			M_n	M_w		
PP	Basell	PP 1	89	288	–	–
PP	Basell	PP 2	166	773	–	–
EPDM	Bayer	EP 1	71.2	141.9	62	4.0
EPDM	Bayer	EP 2	112.4	194	52	4.3
EPDM	Bayer	EP 3	146	241.1	53	4.3

Table 2
Rheological property ratios at constant shear rate and constant shear stress

#	Blend components		Blend name	Torque ratio	At constant shear rate		Matrix shear stress (kPa)	At constant shear stress	
	Dispersed phase	Matrix			p^a	ψ^b		p^a	ψ^b
1	EP 1	PP 2	EP 1/PP 2	0.7	0.7	0.5	90.9	0.5	0.7
2	EP 2	PP 2	EP 2/PP 2	1.3	1.5	1.0	90.9	2.0	0.8
3	EP 3	PP 2	EP 3/PP 2	2.0	2.5	2.0	90.9	5.5	0.8
4	EP 1	PP 1	EP 1/PP 1	4.0	5.0	6.5	11.7	12.0	1.0
5	PP 2	EP 1	PP 2/EP 1	1.4	1.5	2.0	69.4	2.5	1.5
6	PP 2	EP 2	PP 2/EP 2	0.8	0.7	1.0	144.7	0.2	1.5
7	PP 2	EP 3	PP 2/EP 3	0.5	0.4	0.5	231.4	–	1.0[c]
8	PP 1	EP 1	PP 1/EP 1	0.3	0.2	0.2	69.4	–	

PS. All the rheological properties are determined at an average shear rate in internal mixer of 26 s^{-1}.
[a] Viscosity ratio based on complex viscosity.
[b] Elasticity ratio based on G'.
[c] By extrapolation of the data.

was estimated using an empirical calibration technique of Marquez et al. [34].

The materials were weighed accurately so that the mixing chamber was filled to 70% of its total volume. At this loading, an optimum interchange between the two chambers of the mixer is observed and there are no stagnant melt areas in the mixer center due to overfilling. The melt blending was carried out under a nitrogen blanket in order to avoid the degradation of the materials due to environmental oxygen. Subsequently, the torque required to mix the blend compositions was noted. After mixing, the melt was carefully taken out of the mixing chamber and was quenched immediately in cold water to freeze in the morphology generated during melt mixing.

In total, four different types of blends over the entire composition range were prepared. The different types of blends prepared together with their rheological property ratios determined at constant shear rate and at constant shear stress are reported in Table 2.

2.4. Irradiation crosslinking

Irradiation crosslinking was carried out in order to fix the EPDM morphology for the PP matrix dissolution and PP continuity experiments. Blends were prepared at four different viscosity ratios over the entire composition range. All these blends, along with the pure materials, were then subjected to γ-irradiation in air with a Cobalt-60 (^{60}Co) source, using a commercial carrier type 8900 irradiator with a dose rate of 25 kGy/h and to an average optimal [35–37] total dose of 154 kGy.

2.5. Dynamic mechanical thermal analysis

A Rheometric Scientific dynamic mechanical thermal analyzer (DMTA) model V was used to measure the glass transition temperatures (T_g) for the pure EPDM, PP materials, and their blends. The blends were first molded into rectangular samples of approximately $64\times12\times2$ mm^3. These samples were then conditioned at 75 °C in a vacuum oven for 3 weeks to relieve any internal stresses in the molded samples. Initially the experiments were performed using a three point bending clamp in a multi-strain single cantilever mode to determine the linear zone and thus the target strain. Based on the results obtained the experiments were then performed in a multi-frequency single cantilever mode at 1 Hz frequency, with a target strain of 0.1%, and at a heating rate of 1 °C/min. The peak in loss modulus with temperature was used for measuring the T_gs.

2.6. Solvent extraction and gravimetry for % continuity

Three samples of approximately $8\times12\times4$ mm^3, weighing about 0.3–0.4 gm were cut from each of the non-crosslinked blends. These samples were kept in 40 ml of fresh cyclohexane solvent in a centrifuge tube for 48 h at room temperature. The tubes were shaken constantly. The samples were dried in a vacuum oven at 60 °C until constant weight was obtained. The samples were then subjected to another wash of fresh cyclohexane and again dried to constant weight. This procedure was repeated until the sample weight from two consecutive washes remained unchanged.

The irradiated blends were cut into 3 mm cubes, in total weighing about 0.1 gm, to achieve faster dissolution of the PP. These samples were boiled in 100 ml of xylene for 45 min to 1 h. The samples were then dried in a vacuum oven to constant weight. These well-dried samples were boiled in fresh xylene and again dried to constant weight. This procedure was repeated until the sample weight from two consecutive washes remained unchanged.

Assuming that the blend is completely homogeneous, the continuity of the respective material in the blend was calculated using the following equation

$$\%\,\text{Continuity of A} = \left(\frac{\text{Wt of A}_{\text{Before Extraction}} - \text{Wt. of A}_{\text{After Extraction}}}{\text{Wt of A}_{\text{Before Extraction}}}\right)\times 100 \quad (1)$$

where 'A' represents the component which has been extracted and whose continuity has to be determined. The values reported are the average of at least three measurements done in this way.

2.7. Characterization of phase morphology

At least two samples from each blend were cut and microtomed under liquid nitrogen using a glass knife to create a plane face. The instrument is a Leica-Jung RM 2065, and 2165 equipped with a Leica LN 21 type cryochamber. The microtomed samples were then subjected to a cyclohexane wash to remove the EPDM phase and were dried completely. The samples were coated with a gold–palladium alloy, and the observations were carried out under a Jeol JSM 840 Scanning Electron Microscope (SEM) operated at a voltage of 15 kV.

The SEM micrographs were analyzed by a semiautomatic method of image analysis (IA), consisting of a digitizing table and in-house developed software, described elsewhere [38]. On an average at least 300 diameters were measured per blend sample. The number average diameter (d_n) and the volume average diameter (d_v) were then calculated based on these measurements. Since the microtome does not necessarily cut the dispersed phase at the equator and also to correct for the polydispersity, the Saltikov [39] correction was applied.

The micrographs for the blends containing PP as their dispersed phase were obtained by tapping mode atomic force microscopy (AFM). The blend specimens were first cryomicrotomed and the subsequent observations were carried out with a scanning probe microscope Dimension 3100 with a Nanoscope IIIa controller from Veeco Instruments. Silicon tips, model RTESP from Veeco, with spring constants of 20–80 N/m and resonant frequency of 320 kHz were used. The tip was oscillated at 98% of the resonant frequency and the engagement on the surface was done at 95% of the free oscillation amplitude. Topographical pictures were taken at 95% of the free oscillation amplitude.

2.8. BET measurement

A Flowsorb 2300 BET instrument was used to measure the surface area of highly continuous specimens in order to measure the pore diameter. The solvent-extracted porous samples from the solvent gravimetry were cut into small rod-like pieces, so that they could be fed into the cell used in BET measurements. Prior to testing, 1 ml of nitrogen was introduced into the equipment for calibration purposes. The blend samples were then analyzed for their total surface area. At least two readings per sample and two samples per blend were analyzed and the average of those readings was taken for further calculations. Now, by considering that the total volume of the pores is equal to that of the extracted phase (V), the total surface area (S) is that of the pore wall, and that the pores are cylindrical in shape, the pore diameter (d) can be readily calculated as,

$$d = 4V/S \tag{2}$$

Further details regarding this technique have been described by Li and Favis [40].

2.9. Matrix dissolution

2.9.1. Complete matrix dissolution

Less than 0.01 gm of the 95 EPDM/5 PP samples were cut from the blend and were completely dissolved in 300 ml of pre-filtered cyclohexane solvent. The solution was then filtered using a 0.8 μm filter membrane. Additional fresh pre-filtered cyclohexane solvent was filtered to insure complete removal of the dissolved EPDM phase. The weight of the filter membrane before and after filtration and complete drying were noted.

Similarly, 0.02 g of the material was cut from 5 EPDM/95 PP irradiated blends. The material was then completely dissolved in 100 ml of pre-filtered xylene by boiling for 30–45 min. The solution was rapidly filtered at 140 °C using a 0.8 μm membrane. Additional hot xylene was passed to assure the complete removal of the PP phase. The weight of the filter membrane before and after filtration and complete drying were noted.

Our calculations show that on an average we were able to retain more than 80% of the dispersed phase and only about 1% of the matrix phase on the membrane in all cases. This amount is more than enough to asses the shape and structure of the dispersed phase.

2.9.2. Partial matrix dissolution

Upon complete dissolution of the matrix, the individual dispersed phase becomes suspended in the solvent. Occasionally, the very high surface area of the dispersed phase and the tacky nature of the polymers at the experimental conditions (as in this case for EPDM), may lead to the agglomeration of the dispersed phase in solution. The agglomeration makes the identification of the nature of the dispersed phase difficult. In such cases the partial removal of the matrix from the surface can expose the dispersed phase without resulting in agglomeration. This technique especially makes sense for elongated dispersed structures and is complementary to the complete matrix dissolution study.

For the partial matrix dissolution study, the microtomed samples of the 5 EPDM/95 PP irradiated blends, pure EPDM, and pure PP were immersed in hot xylene for about 2–5 s. That time was found to be just enough for the partial dissolution of the PP matrix. These treated samples were rapidly rinsed with cold xylene and later dried in a vacuum oven. The samples were then coated and examined by SEM microscopy.

2.9.3. Complete matrix dissolution of highly continuous blends and freeze drying

In these experiments, initially, small samples were cut from the 30 EPDM/70 PP irradiated blends and 70 EPDM/30 PP non-irradiated blends, the compositions at which the samples present partial continuity. The 30 EPDM/70 PP irradiated blend samples were boiled in xylene to completely remove the PP matrix. Two to three similar washes were given to the sample to assure complete matrix phase removal. After the final xylene wash, the samples were washed several times with cyclohexane. The excess cyclohexane was removed, keeping only just enough solvent to submerge the sample completely.

In the case of 70 EPDM/30 PP non-irradiated blend samples, the EPDM matrix was completely removed by dissolving it in cyclohexane.

All the above samples were subsequently frozen and freeze-dried completely by applying vacuum and by maintaining the temperature of the samples from −25 to −30 °C. These freeze-dried samples were later coated with the gold–palladium alloy and observed under the SEM.

3. Results and discussion

3.1. Rheology

PP and EPDM are known to follow the Cox-Merz [41] relation [5,42], thus the frequency of the rheometer can be directly converted to the shear rate and the complex viscosity can be treated as a steady shear flow viscosity. Fig. 1(a) and (b) shows the complex viscosity and the storage modulus as a function of shear rate. Fig. 1(a) shows that all the materials demonstrate shear thinning behavior. EP 1 and PP 1 and 2 possess a Newtonian plateau. For the higher molecular weight EP 2 and 3 the plateau occurs at a lower frequency than the measured frequency range due to the high relaxation time. At the average shear rate of blending, it can be seen that, EP 3 is the most viscous and most elastic of all the polymers. PP 2 is almost as elastic as that of EP 2 but is less viscous than EP 2. PP 1 is the least viscous and elastic of all the neat polymers.

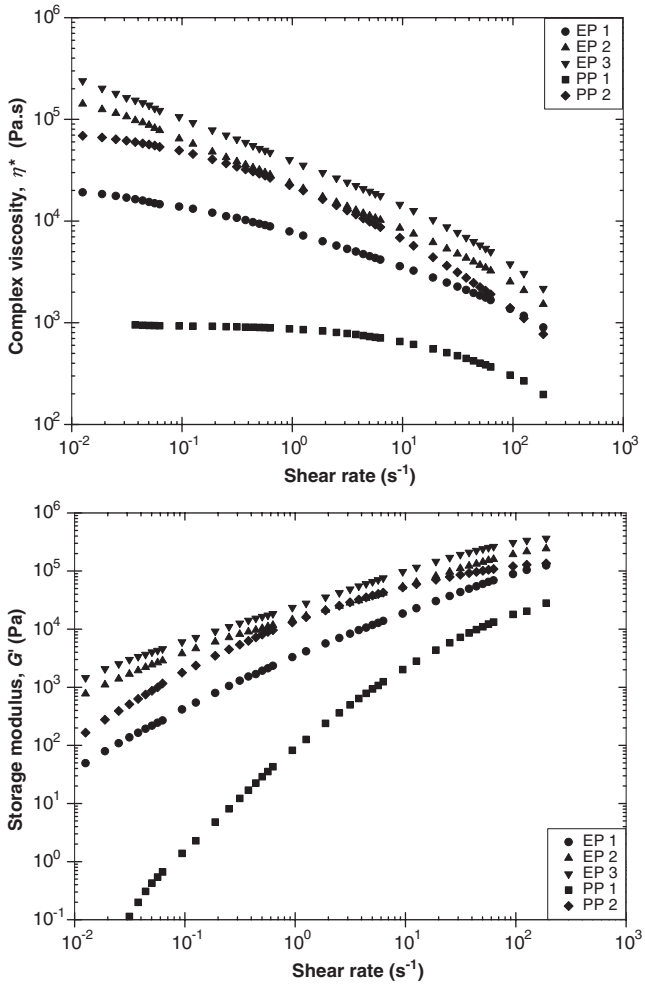

Fig. 1. (a) Complex viscosity of the pure materials as a function of shear rate at 190 °C, (b) Storage modulus of the pure materials as a function of shear rate at 190 °C.

Table 2 shows the blend rheological properties, based on the neat materials, at both constant shear rate and constant shear stress. In the field of polymer blends, there is still some debate as to whether the rheological property ratios should be calculated at constant shear rate or at constant shear stress since the local shear rate at the surface of the droplet under deformation may be discontinuous (although the velocity may be continuous). The local shearing stress may also be discontinuous, if we take into consideration the slip at the interface. Thus, it may be more precise to compare the rheological properties at constant shear stress. Comparing the numbers reveal that no matter how the rheological ratios are estimated, the trends are identical.

3.2. Interfacial tension and miscibility/immiscibility

The interfacial tension between EPDM and PP is known to be very low and is dependent on ethylene content in EPDM, besides other known variables. The weak optical contrast and low interfacial tension makes the actual measurement of the interfacial tension extremely difficult using common experimental techniques. Interfacial tension values ranging from 0.06 to 0.6 mN/m estimated using the harmonic mean equation [43] and various other techniques can be found in the literature [1–6]. Using our own calculation from the harmonic mean equation and considering other data published in the literature, we estimate the interfacial tension between EPDM and PP to be around 0.3 mN/m at the melt blending temperature of 190 °C.

The breaking-thread experiment was also carried out to measure the interfacial tension between these two polymers, however the PP thread in the EPDM matrix did not break up even after several hours. This highly stable thread behavior occurs as a result of the very low interfacial tension between EPDM and PP and can be explained directly from Tomotika theory [44] as outlined in other work [33,45–48]. This result is also a support for the observation of highly stable fibers that will be discussed later in this paper.

As mentioned earlier in the Introduction, the issue of miscibility/immiscibility in this blend system is quite complex and is known to depend on various factors. Thus, it is crucial to determine if the blends in this study show some degree of miscibility between the components. In order to evaluate the miscibility, the T_gs of the lowest molecular weight pure materials and their blends, i.e. of EP 1, PP 1, and their blends, were measured using the DMTA and the results are shown in Fig. 2. It can be seen that the T_g of PP 1 remains completely unaffected by blending. The T_g of EP 1, however, can be seen to decrease as the composition of EP 1 in the blend decreases. Thus, unlike completely miscible systems in which the blends show a single T_g for both blend components (as indicated by the solid line in Fig. 2 and predicted using the Fox equation [49]), or for a partially miscible system [32] in which

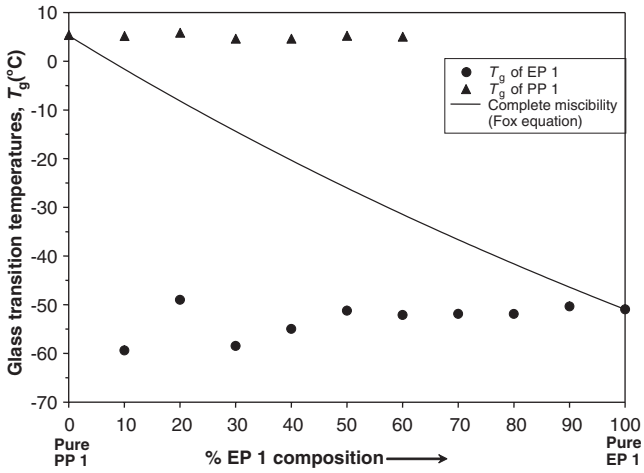

Fig. 2. Glass transition temperatures for the EP 1/PP 1 blends as a function of EP 1 composition in the blend.

the blends show two intermediate T_gs, the T_gs in EPDM/PP blends remain unchanged for PP, and actually decrease with respect to pure EPDM.

Mäder et al. [50] have observed similar phenomenon of T_g depression of styrene–ethylene–butylene–styrene (SEBS), and poly(ethane-*co*-1-octene) (EO) elastomers melt blended with PPs of different stereoregularities. No change in the T_g of any PP was observed on melt blending with an elastomer, however the depression in the T_g of an elastomer was found on melt blending. The effect was more pronounced in the PP with the highest degree of crystallinity, i.e. for *i*PP, and was attributed to thermally induced internal stress resulting from the differential volume contraction of the two phases during cooling from the melt.

It is important to mention here that improper conditioning of these blends prior to T_g measurement, via DMTA testing, can result in erroneous data. The samples used in the above tests and shown in Fig. 2 were conditioned in a vacuum oven for about 3 weeks at 75 °C. A shorter conditioning time resulted in lower T_g values for the PP phase. Blends rich in PP showed the greatest decrease in PP T_g values with the effect becoming progressively less pronounced as the EPDM composition in the blend increased. The T_g values for the EPDM phase, however, did not show any difference on sample conditioning. This decrease in the T_g of the PP phase due to an incomplete conditioning prior to measurement could potentially be erroneously interpreted as a partial miscibility. The relaxation of the frozen-in stresses of the PP phase in the blend, generated during the compression-molding preparation of the samples after blending, thus require a long conditioning time.

The results in Fig. 2, with long conditioning times, clearly demonstrate that the blends with lowest molecular weight EP 1 and PP 1 are completely immiscible and do not show signs of even a partial miscibility at room temperature. By extrapolation, the other higher molecular weight blends would also be expected to show complete immiscibility as the blending technique and the ethylene content of the EPDM elastomer remains unchanged.

3.3. Microstructure of EPDM/PP blends

3.3.1. EPDM minor phase

Micrographs of the EPDM minor phase in EP 1/PP 2 blends (viscosity ratio 0.7 and shear stress 90.9 kPa), at various compositions, are shown in Fig. 3. The minor phase was extracted with cyclohexane. All the micrographs distinctively show a very clear interface between EPDM and PP, which suggests and supports our previous finding that these blends are completely immiscible at room temperature at all compositions. At 10% EPDM, Fig. 3(a), fine particles ranging from 50 to 150 nm are observed. These structures are even finer than those typically reported in the literature [17–22]. As the concentration of the EPDM phase is increased to 20% it can be seen in Fig. 3(b) that the shape of the phases appear to be significantly deviating from the spherical. At 30% in Fig. 3(c) this effect becomes much more pronounced. Finally at 50% the blend reaches the co-continuous morphology as evident in Fig. 3(d). These results clearly point to the importance of confirming the shape of the EPDM phase and that work is outlined below.

Typically in the literature, low concentrations of dispersed EPDM in PP blends are considered to be composed of spherical droplets dispersed in a PP matrix [18–20,51–54]. However, it is very difficult to infer the shape of the minor phase from 2-dimensional micrographs. In order to assess the shape of the dispersed EPDM, a protocol was developed to selectively remove the PP matrix. This is accomplished by irradiation crosslinking the dispersed EPDM phase followed by dissolution of the PP phase with xylene. Results for the matrix dissolution test for systems EP 1/PP 2 and EP 1/PP 1 at 5 and 30% EPDM composition are shown in Fig. 4. Note that upon collection of the 5% dispersed EPDM phase on the filter, it is impossible to avoid agglomeration of the EPDM phase. The very high surface area of the dispersed phase, the tacky nature of EPDM, and the high temperatures used for dissolving the PP matrix in xylene are some of the reasons behind this agglomeration of the particles. Nevertheless, high magnification micrographs of the agglomerate surface in Fig. 4(a) and (b) indicate that it is composed of very uniform fibers of EPDM with dimensions in the 100–200 nm range. At 30% EPDM, the PP matrix dissolution test results in an intact, non-disintegrated structure clearly possessing a very high level of interconnected fibers for both EP 1/PP 2 and EP 1/PP 1. In all cases in Fig. 4, the scale of the fiber diameter corresponds closely to that observed in Fig. 3 for EP 1/PP 2 blends.

In order to further support the observation of EPDM fibers, a partial-PP matrix dissolution was carried out. This allows one to observe the EPDM structure and avoid any EPDM fiber agglomeration. The results of partial matrix dissolution are shown in Fig. 5 for pure EPDM, pure PP and for the 5 EP 1/95 PP 1 system at two magnifications. The PP 1 system was used here since it was easier to control the partial dissolution experiment. Fig. 5(c) and (d) shows elongated fibers of the same scale as seen in Fig. 4(b).

These results clearly indicate, in the viscosity ratio range used in this work, that the dispersed EPDM phase in EPDM/PP

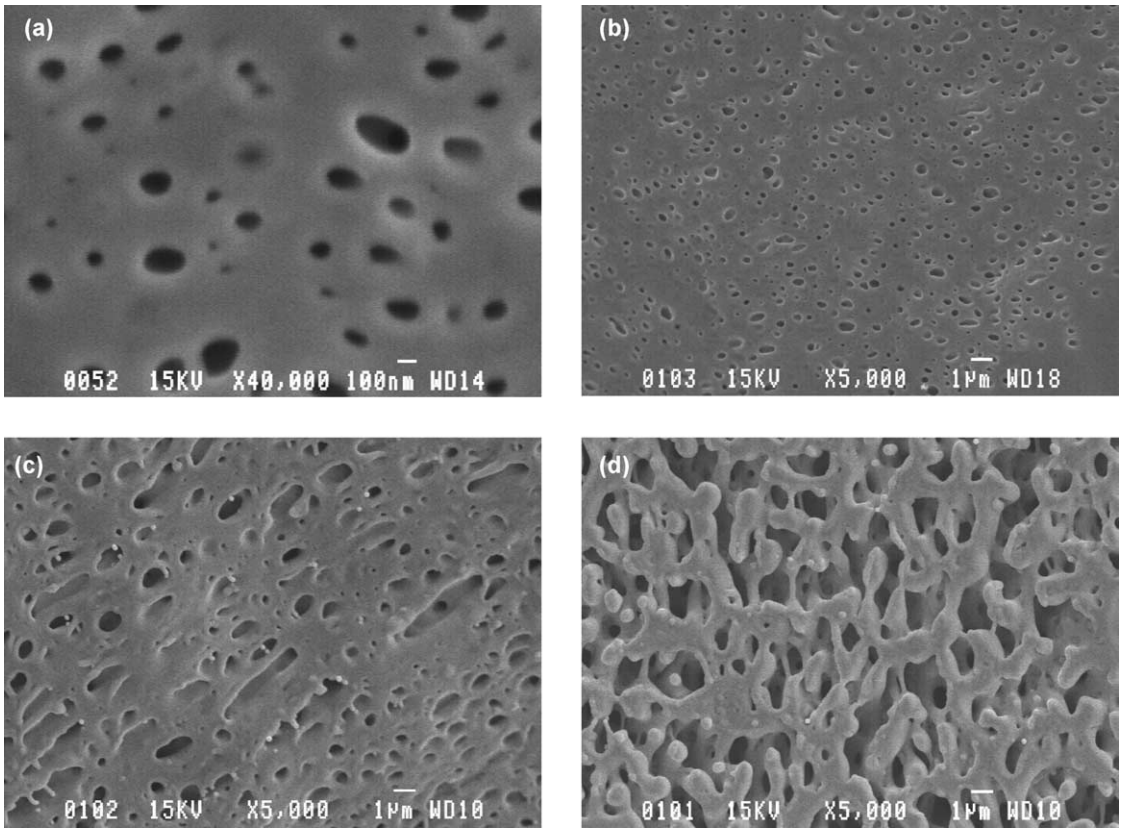

Fig. 3. EPDM phase morphology development. SEM micrograph (a) 10 EP 1/90 PP 2, (b) 20 EP 1/80 PP 2, (c) 30 EP 1/70 PP 2, and (d) 50 EP 1/50 PP 2.

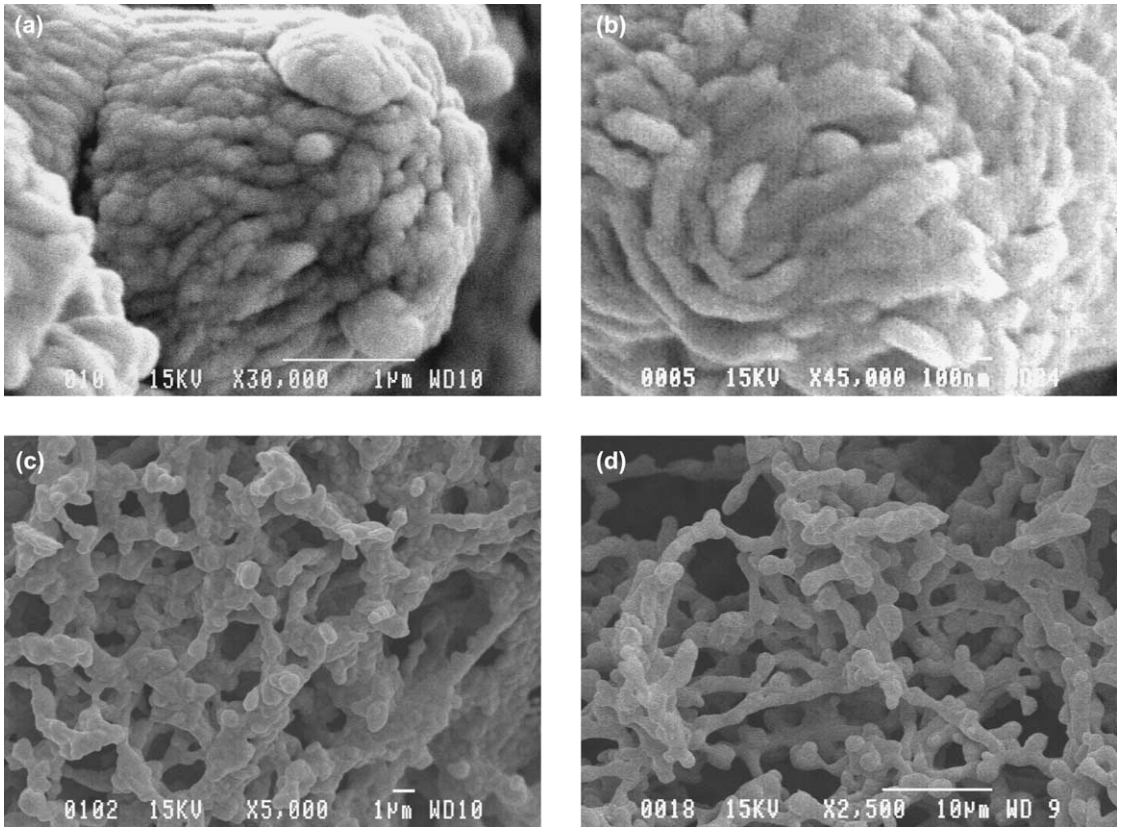

Fig. 4. SEM micrographs of the dispersed EPDM phase after PP matrix dissolution. SEM micrograph (a) 5 EP 1/95 PP 2, (b) 5 EP 1/95 PP 1, (c) 30 EP 1/70 PP 2, and (d) 30 EP 1/70 PP 1.

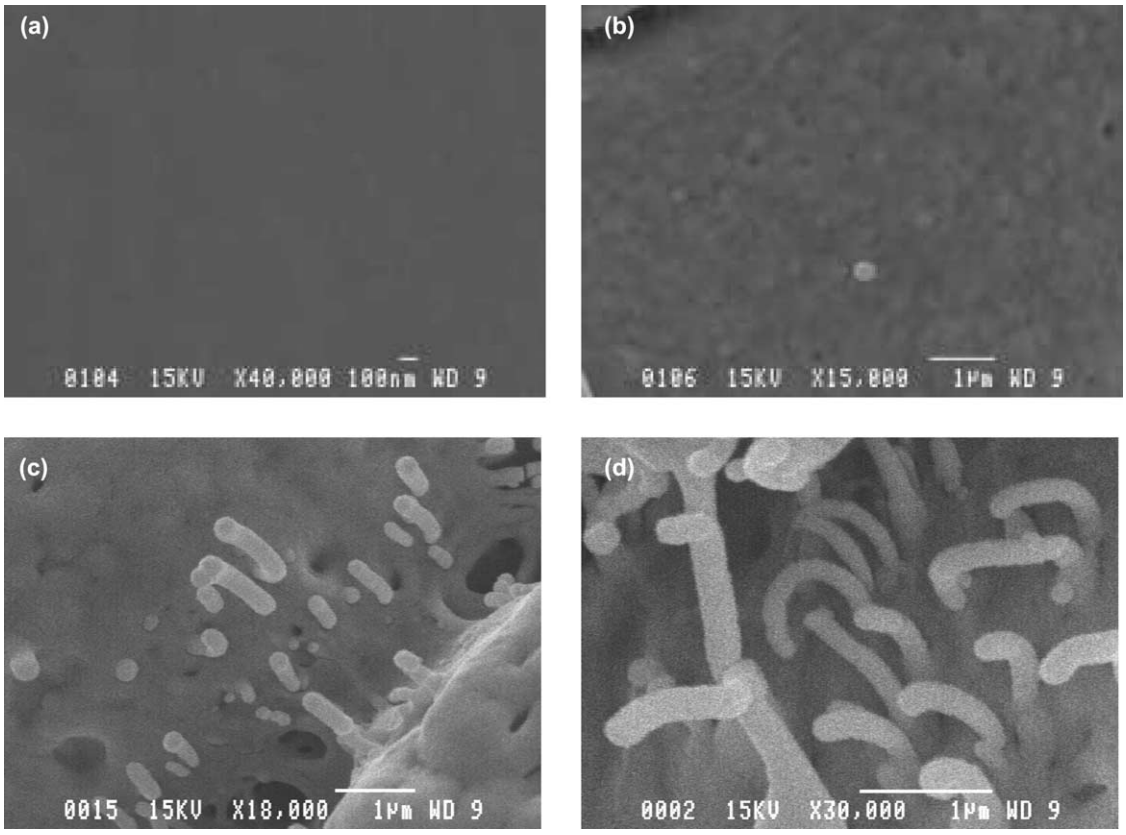

Fig. 5. SEM micrographs after partial PP matrix dissolution. SEM micrograph (a) Pure EP 1, (b) Pure PP 1, (c) and (d) 5 EP 1/95 PP 1.

blends forms nano-scale fibers and challenges the current view of EPDM being dispersed as spherical particles in PP [18–20,51–54].

Tomotika [44] theory also provides theoretical support for this observation. From Tomotika's theory the typical thread breakup time of a Newtonian fluid in the matrix of another Newtonian fluid is given by,

$$t_b = \frac{2\eta_c R_0}{\Omega_m(\lambda_m, p)\sigma} \ln\left(\frac{0.81R_0}{\alpha_0}\right) \quad (3)$$

where t_b is the thread breakup time, η_c is the viscosity of the continuous (matrix) phase, η_d is the viscosity of the dispersed (thread) phase, p is the viscosity ratio (η_d/η_c), R_0 is a initial thread radius, σ is the interfacial tension, $\Omega_m(\lambda_m,p)$ is a complex function of wavelength (λ) and viscosity ratio (p) determined at a dominant wavelength (λ_m), and α_0 is the original amplitude.

In order to theoretically estimate the breakup time we need to estimate the original amplitude α_0. Elemans et al. [47] suggested that α_0 can be estimated from the equation derived by Khun [55] based on fluctuations of the interface caused by Brownian motion. These are the smallest possible perturbations and are always present on a fluid cylinder. Thus Eq. (3) can be re-written as,

$$t_b = \frac{\eta_c R_0}{\Omega_m(\lambda_m, p)\sigma} \ln\left(\frac{1.39\sigma R_0^2}{kT}\right) \quad (4)$$

where k is the Boltzmann constant, and T is the absolute temperature.

The values used for the estimation of the fiber breakup time for both 5 and 10% EPDM in EP 1/PP 2 and EP 1/PP 1 blends are reported in Table 3. The actual average diameter values determined by image analysis at those compositions are used in these calculations. The omega function is determined using the equations developed by Tomotika [44] and by inserting the Bessel function values of $I_n(x)$ and $K_n(x)$ from the tables given by Watson [56], as suggested by Tomotika. The estimated values of the fiber breakup time in Table 3 vary from 7 to 15 min and support the notion of stable EPDM fiber formation over the melt mixing times used in this work. Note that in order to support the experimental breaking thread experiment on a PP thread in EPDM discussed earlier, the theoretical breakup time for a 30 µm PP 2 thread in an EP 1 matrix is also calculated. The extremely long thread breakup times clearly support the experimental observation of no breakup after several hours for this system.

It is well known that Tomotika theory was developed for Newtonian fluids and does not account for complex viscoelastic effects. However, it has been reported that as particle sizes or fiber diameters approach one micron, viscoelastic effects become negligible [57]. As dispersed structures become very small in size, their surface to volume ratio becomes so large that interfacial mechanisms such as capillary instabilities can be expected to dominate breakup over bulk-dominated mechanisms related to viscoelasticity.

Table 3
Estimated fiber breakup times

System	EP 1/PP 2		EP 1/PP 1		PP 2 thread in EP 1 matrix
% EP in the blend	5%	10%	5%	10%	
D_0 (μm)	0.11	0.19	0.44	0.46	≈30
$\eta_{0,EP}$ (kPa)	30.6	30.6	30.6	30.6	30.6
$\eta_{0,PP}$ (kPa)	79.6	79.6	0.96	0.96	79.6
p	0.38	0.38	31.9	31.9	2.6
σ (mN/m)	0.3	0.3	0.3	0.3	0.3
k (kg m^2/s^2 °K)	1.38×10^{-23}	1.38×10^{-23}	1.38×10^{-23}	1.38×10^{-23}	1.38×10^{-23}
T (°C)	190	190	190	190	190
Ω_m (λ_m,p)	0.173	0.173	0.009	0.009	0.06
t_b (s)	446	931	651	688	422,548
t_b (min)	7.4	15.5	10.9	11.5	7042.5

3.3.2. PP minor phase

Similar studies were carried out to demonstrate the PP microstructure in the EPDM matrix, and the results are shown in Fig. 6 for the PP 2/EP 1 system. Since dissolution of the dispersed PP phase is difficult and because of EPDM matrix swelling (which could alter the blend morphology, especially the phase sizes), atomic force microscopy was used to study the morphology of dispersed PP blends. The AFM micrograph (a) for 10 PP 2/90 EP 1 blend shows that the PP, like EPDM, is also distributed uniformly and finely with size scales ranging from 150–300 nm. Moreover, an EPDM matrix dissolution protocol, shown in Fig. 6(b), confirms that the PP phase is also dispersed in the form of nano-meter scale fibers (≈200 nm in diameter). Complete matrix dissolution for the 30 PP 2/70 EP 1

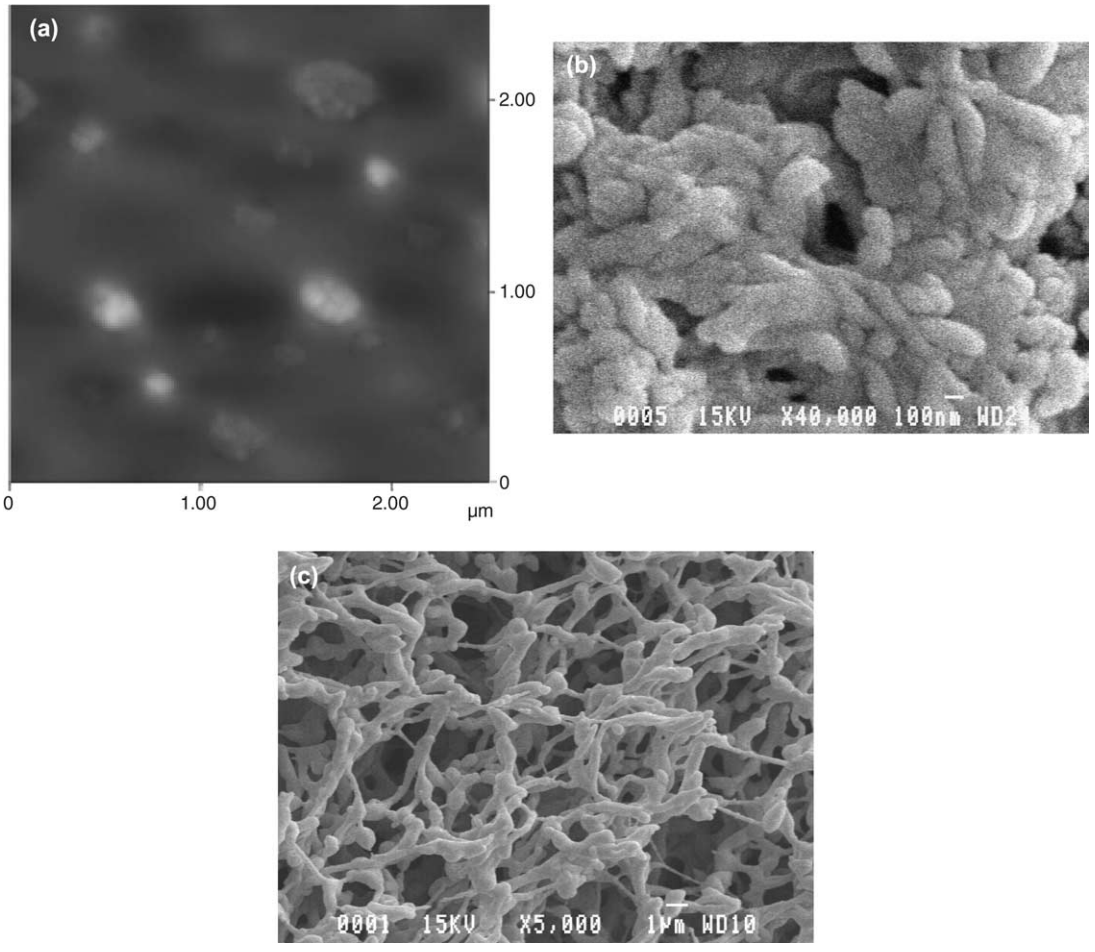

Fig. 6. PP phase microstructure in EPDM matrix. Micrograph (a) atomic force micrograph of 20 PP 2/80 EP 1 blend; SEM micrograph of PP dispersed phase after complete EPDM matrix dissolution in (b) 5 PP 2/95 EP 1 blend, and (c) 30 PP 2/70 EP 1 blend.

blend, Fig. 6(c), shows a network of interconnected PP fibers. This result supports the notion, as observed for dispersed EPDM, that PP continuity develops by fiber–fiber coalescence. The similarity of the microstructural results for dispersed EPDM and dispersed PP are not unexpected since the viscosity and elasticity ratios are not greatly different after phase inversion (see Table 2). The morphology thus appears to be largely dominated by the low interfacial tension.

3.4. Effect of EPDM composition on phase size

Fig. 7 presents the number average and volume average diameters obtained by image analysis as well as the pore diameter obtained by the BET nitrogen adsorption technique as a function of composition for EP 1/PP 2 blends. The system clearly demonstrates high coalescence features as characterized by a 6–10-fold increase in the phase sizes. Coalescence on this scale is highly unexpected for such a low interfacial tension system and this will be discussed along with some anomalies in the continuity data later in Section 3.7.

3.5. Effect of viscosity ratio and matrix viscosity on microstructure

Fig. 8 shows the effect of viscosity ratio and matrix viscosity on the particle size as a function of EPDM composition. All the blends irrespective of their viscosity ratio and matrix shear stress show a significant increase in particle size with composition as shown in the previous section. The viscosity ratio has little effect on the microstructure, however, an eight-fold decrease in the matrix viscosity, i.e. for EP 1/PP 1 blends, does impact the phase sizes by roughly 3 to 4 times at low compositions of EPDM. The strong phase size increase beyond 20% EPDM for EP 1/PP 1 blends is most likely related to the effect of PP viscosity on EPDM coalescence [58–61]. Note however that the matrix viscosity does not significantly influence the shape of the dispersed phase i.e. the EPDM exists as elongated fibers as already shown in micrograph (b) of Fig. 4 for the EP 1/PP 1 blend system.

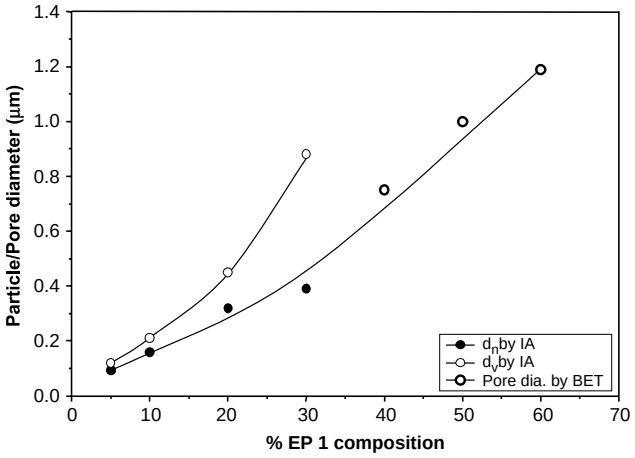

Fig. 7. Average particle/pore diameters as a function of composition for EP 1/PP 2 blends (IA stands for image analysis).

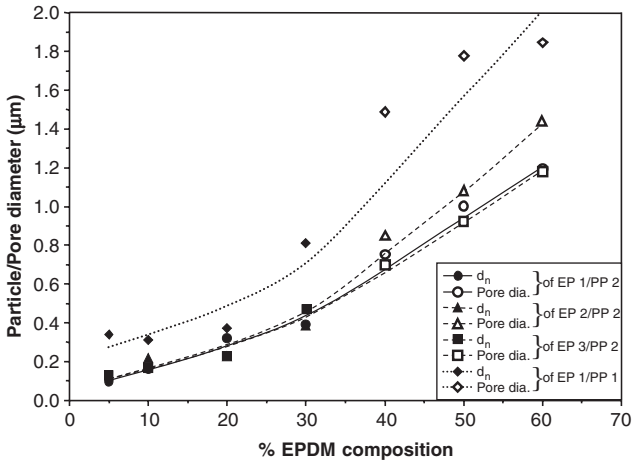

Fig. 8. Effect of viscosity ratio and shear stress on average particle/pore sizes as a function of composition d_n obtained by image analysis and pore diameter by BET.

3.6. Continuity development and co-continuity

Fig. 9 presents the complete continuity development and co-continuity data with composition for EPDM/PP blends at all viscosity ratios. The continuity values reported in this diagram are already corrected for the PP solubility in cyclohexane (about 2.6% for PP 1 and 1.4% for PP 2) at room temperature, and EPDM solubility in boiling xylene (about 3.0%). The correction for PP arises due to the fact that commercial PP contains a small atactic portion or low molecular weight chains of PP, which are soluble in cyclohexane at room temperature. For EPDM the correction is related to the presence of a small fraction of non-crosslinkable EPDM and the gel content achieved by irradiation, since irradiation also causes chain scission of EPDM to some degree. These corrections are necessary, especially at the higher concentration of each component where small amounts of solubility of the major component can result in substantial changes in the continuity values of the minor component.

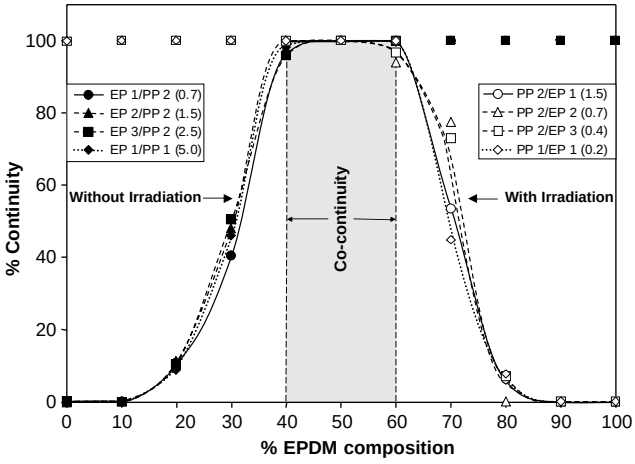

Fig. 9. Complete continuity development and co-continuity diagram for EPDM/PP blends system (corrected for PP solubility in cyclohexane at room temperature, and EPDM solubility in xylene).

Fig. 9 reveals that the continuity development with composition is symmetrical in all EPDM/PP blends studied here. In general, at viscosity ratios between 0.7 and 5.0 and for shear stresses varying from 11.7–90.9 kPa, a virtual single master-curve for continuity development is obtained. There are some differences in the continuity data at 70% EPDM however, the continuity data at that concentration was particularly challenging to measure due to the combination of crosslinked EPDM matrix swelling and the extreme concentration sensitivity of continuity development. The systems demonstrate high percolation thresholds, gradual continuity development and attain co-continuity at high compositions of the minor phase. Co-continuity is maintained over a relatively restricted composition range (about 20 composition units). This behavior is highly unexpected from such a low interfacial tension system. Low interfacial tension systems are known to possess very broad regions of co-continuity [33,45,46]. These anomalies in the continuity data and the higher coalescence already seen in Section 3.4 are explained below.

3.7. Morphological characteristics of partial miscibility

The EPDM/PP system, according to a definition provided by Li et al. [33], represents a Type I low interfacial tension binary blend. In fact the EPDM/PP system has an even lower interfacial tension than that of the styrene–ethylene–butylene–styrene (SEBS)/high density polyethylene (HDPE) blends system studied by Li et al. This type of system is expected to demonstrate: a dispersed phase in the form of very uniform fibers and thus continuity development by fiber–fiber coalescence; very low percolation thresholds; and attainment of co-continuity at low compositions. Moreover, they showed that these systems possess a very large composition range for co-continuity and virtually no dependence of phase size with composition. Although this system demonstrates some of the expected features of a low interfacial tension immiscible binary blend such as low diameter fiber formation and continuity development via fiber–fiber coalescence (Figs. 4–6), a number of anomalies are also observed, i.e. the EPDM/PP system shows a dependence of pore size with composition in Figs. 7 and 8; high percolation threshold compositions as shown in Fig. 9; and a composition range for dual-phase continuity of only 20 composition units. These latter characteristics are more typical of a high interfacial tension blend system.

As mentioned earlier, Marin et al. [32] observed similar tendencies for a low interfacial tension PMMA/PC system. They were able to relate those deviations to the partial miscibility of PMMA/PC. In a detailed study of glass transition temperatures for the PMMA/PC blend they were able to quantitatively estimate the extent of partial miscibility using the Fox equation [49] and correct the gravimetric data by considering the blend as a mixture of a PMMA-rich phase with a PC-rich phase. By correcting the continuity and co-continuity data in this way they were able to demonstrate that the blend showed all the principal features of a low interfacial tension system: very low percolation thresholds and low concentration for the attainment of fully co-continuous structures. They related the increase in phase size with increasing composition to a reduced miscibility of the PMMA/PC system.

The anomalies seen in this research work for EPDM/PP blends closely correspond to the behavior of partially miscible systems, yet Fig. 2 shows that these blends are completely immiscible upon cooling from the melt. Unlike the partially miscible PMMA/PC system, the main difference in this work, however, is that PP is a crystallizable component. The blends studied in this work thus present the morphological characteristics of a mixture, which was partially miscible during melt blending at which time the gross morphological features are developed. The crystalline nature of PP then drives the system to complete phase separation upon cooling. It appears, however, that the quenching of the EPDM/PP blend from the melt is rapid enough to preserve the imprint of that partial miscibility on the gross blend morphology.

Since the blends completely phase separate upon cooling, the quantitative estimation of the extent of partial miscibility using the Fox equation and subsequent corrections to the gravimetric data in Fig. 9 are not possible for this EPDM/PP blend system.

4. Conclusions

This research work studies continuity development and co-continuity in very low interfacial tension EPDM/PP blends. Blends with viscosity ratios of 0.2–5.0 and shear stresses of 11.7–231.4 kPa are considered.

In contrast to the current view of the dispersed phase in EPDM/PP blends as being in the form of spherical droplets, it is demonstrated that the minor phase (of either components) is dispersed in the form of extremely small diameter stable fibers (50–200 nm). These fibers are shown to coalesce together at crossover points to develop the continuity and co-continuity as per the expected behavior of a binary compatible system.

The blends demonstrate virtually no effect of a seven-fold variation in the viscosity ratio on a range of features including: the phase size, shape of the dispersed phase, % continuity and region of co-continuity. However, an eight-fold variation in shear stress does affect the particle size.

The complete continuity diagram shows a very symmetrical continuity development for either of the blend components. The blends present high percolation thresholds, gradual continuity development, and attainment of co-continuity at high compositions of the minor phase. The blends also demonstrate unusually high levels of coalescence with composition of minor phase, for such a low interfacial tension system. The morphological features of this blend strongly indicate that the blends were partially miscible in the melt; however, the crystalline nature of PP forces the blends to completely phase separate upon cooling, as shown by the glass transition temperatures of the quenched blend samples. The quenching of the blends from the melt is clearly rapid enough to preserve the imprint of the partial miscibility in the melt on the gross blend morphology.

Acknowledgements

The authors would like to thank Mr Mike Gallagher of Bayer Inc. for supplying the EPDM; Mr Denis Therrien of Basell Polyolefins Inc. for supplying and measuring the molecular weights of the PP; Prof Monique Lacroix, of the INRS-Institut Armand-Frappier, Université du Québec, for irradiating the blends; and Mr Pierre Sammut, and Ms Nicole Côté of the Industrial Materials Institute of the National Research Council of Canada for their kind assistance with the DMTA. The authors would also like to thank the 'Groupe de Mélanges Polymères' of École Polytechnique de Montréal, and especially Nick Virgilio for the AFM and Xavier Roy for his kind expertise in freeze drying.

References

[1] Mighri F, Huneault M. Can J Chem Eng 2002;80(6):1028–35.
[2] Reichart GC, Graessley WW, Register RA, Krishnamoorti R, Lohse DJ. Macromolecules 1997;30:3036–41.
[3] Pogodina NV, Chapman BR, Lohse DJ. PMSE Prepr 2003;89:421–3.
[4] Tsou AH, Lyon MK. ANTEC Proc 58th Annu Tech Conf, Soc Plast Eng 2000;58(2):2116–9.
[5] Chung O, Coran AY. Rubber Chem Technol 1997;70(5):781–97.
[6] Hemmati M, Nazokdast H, Shariat Panahi H. J Appl Polym Sci 2001; 82(5):1129–37.
[7] Yamaguchi M, Miyata H, Nitta K. J Appl Polym Sci 1996;62(1):87–97.
[8] Chen CY, Yunus WMdZW, Chiu HW, Kyu T. Polymer 1997;38(17): 4433–8.
[9] Amash A, Zugenmaier P. J Polym Sci, Polym Phys 1997;35(9):1439–48.
[10] Ramanujam A, Kim KJ, Kyu T. Polymer 2000;41:5375–83.
[11] Xiao HW, Huang SQ, Jiang T, Cheng AY. J Appl Polym Sci 2002;83: 315–22.
[12] Zhao R, Dai G. J Appl Polym Sci 2002;86:2486–91.
[13] Fischer WK. US Patent 3,806,558; 1974.
[14] Coran AY, Das B, Patel RP. US Patent 4,130,535; 1978.
[15] Abdou-Sabet S, Fath MA. US Patent 4,311,628; 1982.
[16] Coran AY, Patel RP. Rubber Chem Technol 1982;55:116–36.
[17] Danesi S, Porter RS. Polymer 1978;19(4):448–57.
[18] Karger-Kocsis J, Kallo A, Kuleznev VN. Polymer 1984;25(2):279–86.
[19] Yang D, Zhang B, Yang Y, Fang Z, Sun G, Feng Z. Polym Eng Sci 1984; 24(8):612–7.
[20] Dao KC. Polymer 1984;25(10):1527–33.
[21] Jang BZ, Uhlmann DR, Vander Sande JB. J Appl Polym Sci 1985;30(6): 2485–504.
[22] D'Orazio L, Mancarella C, Martuscelli E. Polymer 1991;32(7):1186–94.
[23] Karger-Kocsis J, Kallo A, Szafner A, Bodor G, Senyei Zs. Polymer 1979; 20(1):37–43.
[24] Martuscelli E, Silvestre C, Abate G. Polymer 1982;23(2):229–37.
[25] Martucelli E. Polym Eng Sci 1984;24(8):563–86.
[26] Lohse DJ. Polym Eng Sci 1986;26(21):1500–9.
[27] Lohse DJ, Wissler GE. J Mater Sci 1991;26(3):743–8.
[28] Han SJ, Lohse DJ, Condo PD, Sperling LH. J Polym Sci, Polym Phys 1999;37(20):2835–44.
[29] Seki M, Nakano H, Yamauchi S, Suzuki J, Matsushita Y. Macromolecules 1999;32(10):3227–34.
[30] Inaba N, Sato K, Suzuki S, Hashimoto T. Macromolecules 1986;19(6): 1690–5.
[31] Inaba N, Yamada T, Suzuki S, Hashimoto T. Macromolecules 1988; 21(2):407–14.
[32] Marin N, Favis BD. Polymer 2002;43(17):4723–31.
[33] Li J, Ma PL, Favis BD. Macromolecules 2002;35(6):2005–16.
[34] Marquez A, Quijano J, Gaulin M. Polym Eng Sci 1996;36(20):2556–83.
[35] Zaharescu T, Setnescu R, Jipa S, Setnescu T. J Appl Polym Sci 2000;77: 982–7.
[36] Kammel G, Wiedenmann R. Siemens Forsch—u Entwickl 1976;5(3): 157–62.
[37] Vroomen GLM, Visser GW, Gehring J. Rubber World 1991;205(2): 23–32.
[38] Favis BD, Chalifoux JP. Polym Eng Sci 1987;27(20):1591–600.
[39] Saltikov SA. In: Elias H, editor. Proceedings of the second international congress for stereology. Berlin: Springer–Verlag; 1967. p. 163–73.
[40] Li J, Favis BD. Polymer 2001;42(11):5047–53.
[41] Cox WP, Merz EH. J Polym Sci 1958;28:619–22.
[42] Chung O, Coran AV, White JL. ANTEC, Proc 55th Annu Tech Conf, Soc Plast Eng 1997;55(3):3455–60.
[43] Wu S. Polymer interface and adhesion. New York: Marcel Dekker Inc; 1982.
[44] Tomotika S. Proc R Soc London 1935;A150:322–37.
[45] Willemse RC, Posthuma de Boer A, Van Dam J, Gotsis AD. Polymer 1998;39(24):5879–87.
[46] Veenstra H, Van Lent BJJ, Van Dam J, Posthuma de Boer A. Polymer 1999;40(24):6661–72.
[47] Elemans PHM, Janssen JMH, Meijer HEH. J Rheol 1990;34(8):1311–25.
[48] Elmendorp JJ. Polym Eng Sci 1986;26(6):418–26.
[49] Fox TG. Bull Am Phys Soc 1956;1(2):123.
[50] Mäder D, Bruch M, Maier R, Stricker F, Mülhaupt R. Macromolecules 1999;32(4):1252–9.
[51] Thamm RC. Rubber Chem Technol 1977;50(1):24–34.
[52] Martuscelli E, Silvestre C, Bianchi L. Polymer 1983;24(11):1458–68.
[53] Karger-Kocsis J, Kiss L, Kuleznev VN. Polym Commun 1984;25(4): 122–6.
[54] Jang BZ, Uhlmann DR, Vander Sande JB. J Appl Polym Sci 1984;29(12): 4377–93.
[55] Kuhn W. Kolloid Z 1953;132:84–99.
[56] Watson GN. A treatise on the theory of Bessel functions. 2nd ed. Cambridge: University Press; 1966.
[57] Van Oene H. J Colloid Interf Sci 1972;40(3):448–67.
[58] Wildes G, Keskkula H, Paul DR. Polymer 1999;40:5609–21.
[59] Roland CM, Bohm GGA. J Polym Sci, Polym Phys 1984;22(1):79–93.
[60] Kressler J, Higashida N, Inoue T, Heckmann W, Seitz F. Macromolecules 1993;26(8):2090–4.
[61] Fortelny I, Zivny A. Polymer 1995;36(21):4113–8.